Voltage-driven class E amplifier and applications

T. Brabetz and V.F. Fusco

Abstract: A voltage-driven class E power amplifier topology is presented. The operating principle of the circuit is explained, and measurement results for a MIC implementation using an OMMIC ED02AH $6 \times 50\,\mu m$ pHEMT as the active device are given. At the nominal operating frequency of 870 MHz, the MIC achieves 18 dB maximum gain, produces 18 dBm output power, and a maximum power added efficiency of 93%.

1 Introduction

The class E amplifier is a highly nonlinear highly efficient switching-class amplifier introduced by N.O. and A.D. Sokal in 1975 [1]. Being a switching amplifier, the class E amplifier is in theory capable of reaching 100% efficiency for maximum output power. In contrast, the class C power amplifier, also capable of in theory 100% efficiency, can only achieve such high efficiency levels for low output power settings [2]. This makes the class E amplifier attractive for mobile power amplification applications, since increased efficiency at high output power levels means longer battery lifetime and less heat dissipation.

Another reason for choosing a switching class amplifier is to make implementation of output power level control easier, for example with a class E amplifier, power level control can in principle be achieved by controlling the bias voltage [3], which has the added advantage that efficiency levels do not suffer as much as they do for conventional linear amplifiers when operated in power back-off mode.

2 Working principle

2.1 Conventional class E design

Figure 1 shows the conventional current driven class E circuit schematic as suggested by Cripps [4]. The active device is represented by the switch, its switching action stimulates an oscillation in the moderate-Q series resonant circuit L_S, C_S tuned close to the RF, thus forcing a sinusoidal current through the load resistor R_L. In parallel with the device is a shunt capacitance C_p, DC bias is applied through an RF choke of sufficient size to sustain constant current throughout an entire RF cycle. The opening and closing of the switch is controlled by the RF input signal's zero crossings, and is therefore to a first approximation independent of the input signal amplitude.

The task of the shunt capacitor C_p (Fig. 1) is to act as a temporary energy store, to allow the series resonant circuit L_S, C_S to sustain a sinusoidal current while the switch is open. The sinusoidal output current, i_θ is either flowing through the switch, i_{sw} while it is closed, or into the capacitor, i_C while the switch is open. If the switch timing and the size of C_p have been chosen correctly, then the shunt capacitor C_p is completely discharged during the negative half-swing of the output current, and the switching is taking place while there is no voltage present over the output terminals of the active device. Hence power dissipation is reduced to zero. In a real class E amplifier the switch timing is set via the gate bias.

In contrast, Sokal's original design [1] uses the same circuit as given in Fig. 1, but the L_S, C_S circuit is used to shape the flanks of the switching waveform rather than the output signal waveform itself. Hence, Sokal's series resonant circuit is tuned to a frequency significantly different to that of the RF signal. Since Sokal's approach relies on the switch being fast with respect to the output signal, its use is restricted to lower frequencies than those obtained if operated according to the principles suggested by Cripps.

2.2 Problems with the conventional design

The class E power amplifier as described in Section 2.1 is well documented in the literature. However, in spite of its potential for 100% efficiency, uptake by industry has been slow so far. This is believed to be the result of a number of factors that will be further examined in this Section.

As mentioned before, the class E power amplifier is inherently nonlinear, since the input waveform controls only the timing of the switch by means of its zero transitions. The switch then stimulates a series circuit to resonate, and consequently the amplitude of the output signal to a first approximation does not depend on the amplitude of the input signal. This property prevents the class E amplifier from being used for systems requiring amplitude modulation. However, since most modern digital modulation schemes are phase modulated, this restriction becomes irrelevant for a number of state-of-the-art communication system applications.

Most significantly, the conventional class E power amplifier suffers from a major technology problem. This occurs owing to the fact that the conventional design is current based, i.e. current waveforms control circuit behaviour. Therefore, the conventional class E power amplifier is inherently sensitive to active device parasitic resistances. The reason for this is that since the currents flowing through the active device are relatively high, even small parasitic resistances cause voltage drops that are large enough to interfere with the ideal operation of the circuit.

IEE Proceedings online no. 20045159

doi:10.1049/ip-map:20045159

Paper first received 17th November 2004 and in revised form 10th February 2005

The authors are with the Institute of Electronics, Communications and Information Technologies, Queen's University Belfast, Northern Ireland Science Park, Queen's Road, Queen's Island, Belfast, BT3 9DT, UK

E-mail: T.Brabetz@ecit.qub.ac.uk

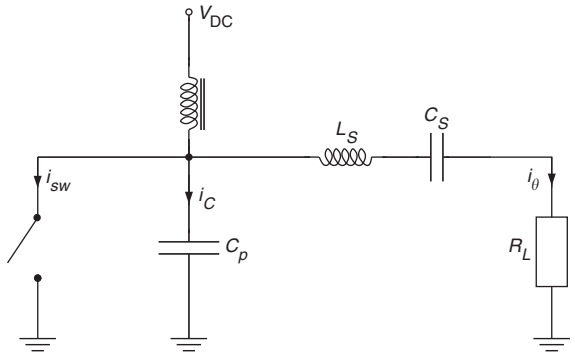

Fig. 1 *Current-driven class E power amplifier circuit schematic [4]*

As a consequence, the majority of all class E microwave designs known to the authors have used HBT's as the active device, since their collector resistances are about a factor of 10 smaller than the drain-source resistance of a typical 100 µm gate width pHEMT. For example, the collector resistance of a $2 \times 10\,\mu m^2$ HBT, capable of providing typically 35 mA collector current for about 1.5 V collector voltage, is about 1.7 Ω [5], while the drain resistance of a comparable pHEMT with 100 µm gate width, typically providing about 40 mA current for 2 V drain voltage [5], is in the range 10–20 Ω. Only for relatively large devices with gate widths in excess of 1 mm does the drain resistance of pHEMTs drop to less than 2 Ω [5].

Furthermore the on-conductance of a pHEMT drain varies with the gate width [5]. The only pHEMT-based class E designs known to the authors feature relatively large devices, with total gate widths in the range 1 mm [6] to 12 mm [3]. For these devices the quoted performance is good (e.g. 90% power added efficiency at 3.25 GHz [6]), but yield, reliability, and compliance with normal GaAs foundry parameters for such large devices have not been stated.

2.3 Voltage-based class E design

To reduce the impact of active device channel resistance on class E power amplifier behaviour, we decided to build a class E amplifier that is controlled by voltage waveforms instead of current waveforms. A voltage-driven circuit was suggested by Raab in 1977 [7], but its detailed properties were not investigated, and moreover it contained a transformer, which is difficult to build at microwave frequencies. In addition, we have been unable to find any references to further work done on this type of circuit. Thus the purpose of this paper is to produce to our knowledge for the first time practical investigations of the characteristics of such a topology.

The authors therefore suggest a simplified version of that given in [7], the topology shown in Fig. 2. Here, the shunt capacitor C_p in Fig. 1 has been replaced by a series inductor L_p. The series resonant circuit L_S, C_S, (Fig. 1) has been replaced with a parallel circuit. This parallel circuit now forces a sinusoidal voltage across R_L and the switch. If the switch is open, i.e. $i_{sw} = 0$, then this sinusoidal voltage builds up over the switch, V_{sw}, since $V_L = di_{sw}(t)/dt$. If the switch is closed, then $V_{sw} = 0$, and the sinusoidal voltage builds up over L_p. The sole task of the capacitor C_B in series with the parallel circuit L_S, C_S is to prevent L_S from shorting the bias voltage, and the bypass capacitor to decouple the bias voltage from the RF signals has been replaced with an RF choke. Hence, the new voltage-based design is the electrical dual of the conventional current-based approach, but does not require a transformer at microwave frequencies.

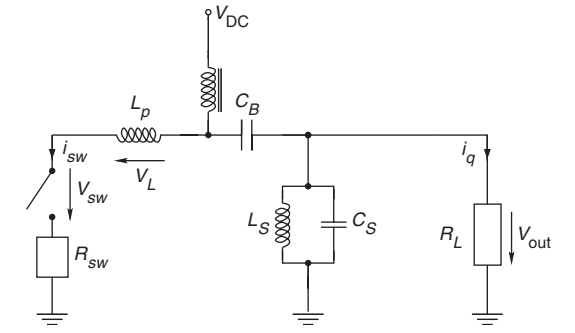

Fig. 2 *Voltage-driven class E power amplifier circuit schematic*

For a voltage-based approach, an important parameter of the active device when used as a switch is its off-resistance, since leakage currents during the off-cycle impair circuit performance. According to Anholt [5], the off-resistance of a HBT used as a switch is virtually infinite, and hence superior to the channel resistance of a pinched-off pHEMT, which is typically in the order of several kΩ. Hence, for low frequencies, performance of HBTs may be superior to that of pHEMTs. However, at the frequencies discussed here, the dominant parameter is the output capacitance, which is around 30 fF for small pHEMT devices, while an HBT has a collector-emitter capacitance of about 40 fF. Hence, during the off-cycle, neither device is vastly superior over the other.

The drain-to-source capacitance of a pHEMT in first approximation increases linearly with total gate width [5]. Hence, with increasing gate width the leakage currents during the off-cycle increase, and the advantage of the voltage-based class E design over the conventional approach is mitigated. In first approximation, the voltage-based approach will cease to be superior to the conventional approach when the decrease in output capacitance during the off-cycle is of similar magnitude to the increased channel resistance during the on-cycle for small devices. Since the channel resistance of small devices is about ten times higher that that of large devices, this point is reached when the output capacitance has approximately tenfold compared to the small devices, which happens at around 1.5 mm total gate length [5].

In conclusion, the voltage-base approach presented here, owing to its inherent robustness against channel resistance, should allow the use of reasonably small pHEMT devices to build high-efficiency class E amplifiers for low-power applications. As total gate width increases, so does the drain-source capacitance, mitigating the positive effects of the voltage-based approach. Owing to these features it appears that the voltage-based approach is particularly suited for circuits with low RF power requirements where intended battery life is important, e.g. applications in the ISM band at 2.4 GHz where EIRP should be less than 100 mW in Europe [8]. With an $8 \times 75\,\mu m$ device (not available to us at the time of construction) our calculations show that at 2.4 GHz, 100 mW at 80% efficiency should be possible.

3 Simulation results

3.1 Evaluation using ideal components

The new topology was first simulated with Agilent's Advanced Design System (ADS) using an ideal switch with an adjustable series resistance R_{sw} (Fig. 2) replacing the active device. Since the switch is an extremely nonlinear component, transient simulation was chosen as the most suitable simulation technique.

Figure 3 compares the waveforms of the new structure Fig. 3*c* with those of the original Cripps design, (Figs. 3*a*, *b*). Figure 3*a* shows, from top to bottom, the switch current i_{sw}, the shunt capacitor current i_C, and the voltage across the shunt capacitor, V_C, respectively. For this simulation, the switch has been stimulated with an internal resistance of 0.1 Ω (an ideal 0 Ω resistance lead to numerical problems) in the closed state.

Figure 3*a* shows how the sinusoidal output current i_θ created by the series resonant circuit L_S, C_S, Fig. 1, is split cleanly into current i_{sw}, and current i_C as long as the switch timing is precise. The switch series resistance in this case is small enough to ensure that i_θ flows exclusively through the switch while it is closed, ensuring that the shunt capacitor C_P is discharged at the moment of switching, bottom graph.

The centre graph shows the same current and voltage waveforms, but this time with a series resistance of 5 Ω for the switch in the closed state. As can be seen, the signals are significantly distorted. Particularly, owing to the higher resistance of the switch, some current flows into the shunt capacitor C_P even when the switch is closed, and therefore the shunt capacitor voltage V_C is no longer zero at the time of switching, causing a spike that upsets circuit operation. The two currents i_{sw} and i_C, when combined, no longer lead to a sinusoidal signal, and the circuit ceases to work properly.

Figure 3*c* shows, from top to bottom, the inductor voltage V_L, switch voltage V_{sw}, and inductor switch current i_{sw}, respectively. The switch has again been set to 5 Ω internal resistance. For the new design, the voltages V_L and V_{sw} complement each other such that, when overlaid on the same scale, they result in the required sinusoidal output signal. Since no spike is created upon switching that could interfere with the circuit timing, the circuit continues to operate in spite of the presence of switch series resistance. Further stimulation has shown that we can increase R_{sw} in Fig. 2 up to 20 Ω without unduly impairing the voltage driven waveform shapes. The new circuit has somewhat different timing characteristics compared to Cripps's design owing to the fact that voltages rather than currents are switched.

4 Class E amplifier MIC

4.1 Circuit description

To confirm these results, we build a hybrid MIC version of the voltage-driven topology (Fig. 4). The circuit was constructed using Taconics TLY-5-0100-CH softboard, mounted on a brass carrier using conductive epoxy to provide mechanical stability. Standard surface-mount components, whose values are defined in Table 1, were used for the passive network, while the active device is an OMMIC ED02AH 6×50 μm pHEMT device. The component values were first obtained using the design equations derived by Cripps [4], and then optimised in Agilent's Advanced Design System (ADS) using transient simulations with a foundry-supplied large-signal model for the pHEMT.

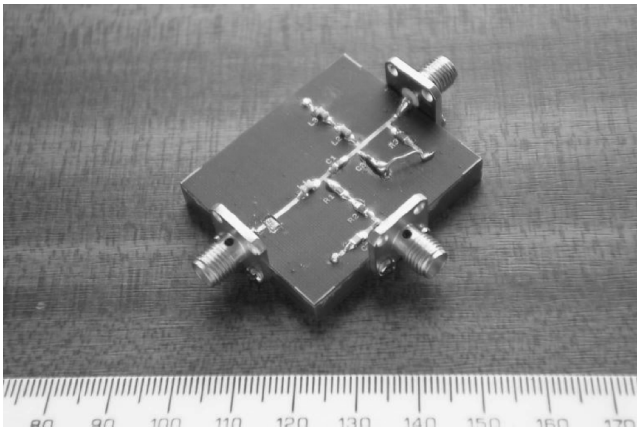

Fig. 4 *Photograph of class-E MIC*

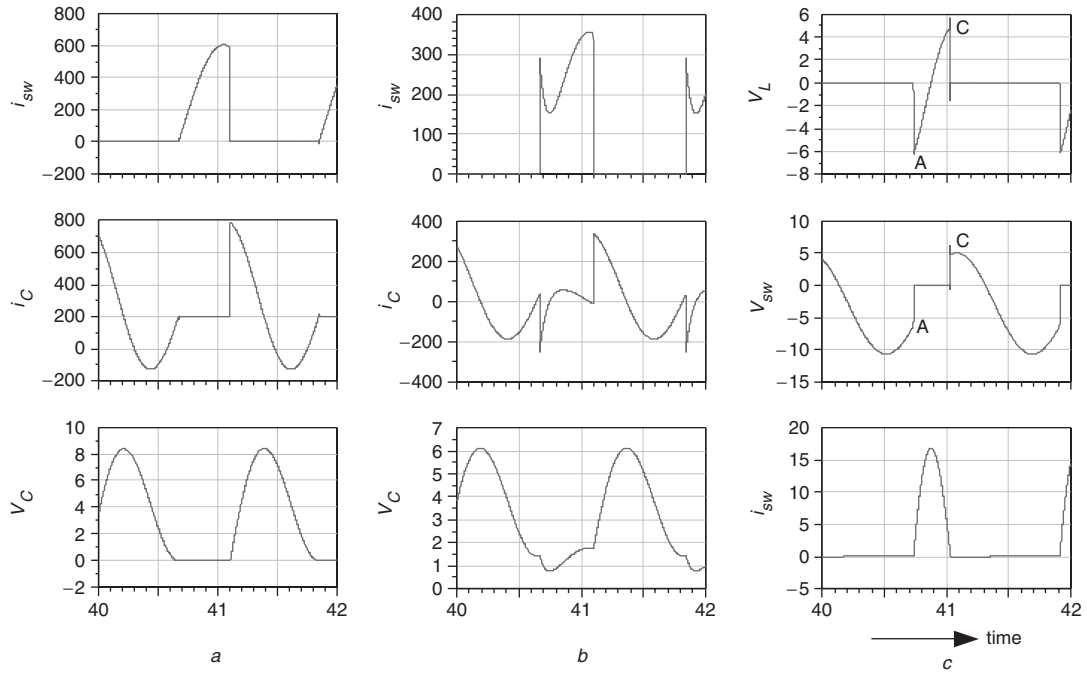

Fig. 3 *Waveforms*
a Ideal switch
b Lossy switch
c Suggested circuit with lossy switch

Table 1: Component values used

Component	Value
L_p	6.5 nH
L_S	37 nH
C_S	1 pF
C_B	47 pF
RF choke	37 nH
Switch	6 × 50 μm pHEMT

The active device has been mounted with conductive epoxy onto a brass pedestal in order to bring its surface level with the TLY-5 substrate, and the electrical connections established using 17.5 μm gold wire-bonds. SMA sockets have been soldered directly onto the TLY-5 microstrip lines to allow the test equipment to be connected. DC gate bias was supplied through the RF_{in} port using a bias tee.

In order to keep the circuit simple, a dedicated output matching circuit was not used, i.e. any matching provided by the L_S, C_S network was not optimised. For the measurements, the input of the amplifier was matched to 50 Ω using Focus Microwaves model 1808 tuners. Owing to the limited tuning range of the tuners, and the highly reactive input impedance of the pHEMT, two tuners were required to achieve a small signal return loss of 20 dB at 870 MHz. The tuning point of the tuners was established empirically to achieve maximum power output for given input power level.

4.2 Measurement results

Figure 5 shows the measurement setup. The input signal was generated using an Agilent HP 8657 B signal generator, capable of providing a maximum of 18 dBm input power at 870 MHz. A drain bias of +2 V is directly supplied to the V_{cc} port of the class E amplifier. Finally, the output signal is fed through a second bias tee to an Agilent HP E 4407 B spectrum analyser. A spectrum analyser was chosen to ensure that the output signal was of acceptable spectral purity, and the amplitude readings of the spectrum analyser were confirmed using an HP 437 B power meter. Figure 6 shows the results obtained with this setup.

At the nominal input power level of 0 dBm, the power amplifier exhibits 17.9 dB gain resulting in an output power of 17.9 dBm (61.7 mW), 95% efficiency and 93% power added efficiency at a frequency of 870 MHz. Bias conditions were +2 V bias voltage, −0.1 V gate bias, and 32.6 mA bias current resulting in 65.2 mW consumed DC power. Harmonic suppression was 37.9 dB for the second

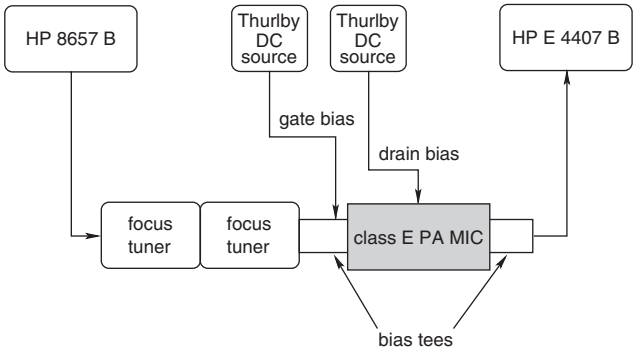

Fig. 5 *Measurement setup*

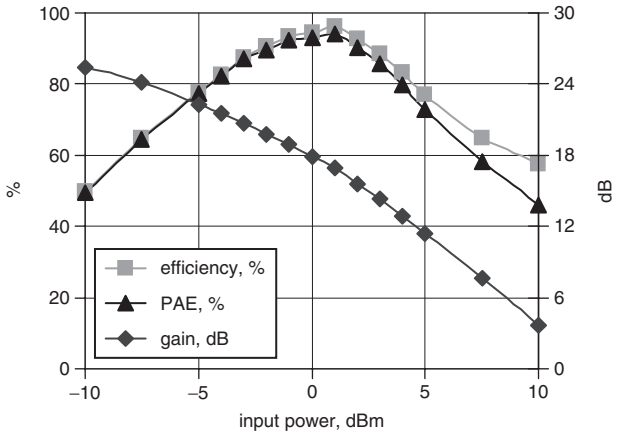

Fig. 6 *Gain, efficiency and power added efficiency against input power at 870 MHz*

harmonic, and 38.4 dB for the third harmonic. For lower input power levels, the amplifier achieves higher gain, e.g. 27 dB for −15 dBm input signal level. However, since the bias current remains virtually unchanged as drive power level is varied, efficiencies under those operating conditions are low at around 24%. Maximum efficiency of 96%, and maximum power added efficiency of 94% are achieved for 1 dBm input power level.

These results, shown in Fig. 6, compare well with the published literature for other pHEMT devices but used in conventional current driven mode, e.g. a class E PA MIC introduced by Nagle *et al.* in 2001 [3], which at 900 MHz exhibited a gain of 9.5 dB, an output power of 31.5 dBm, and a PAE of 53%, however using a much larger device having 12 mm total gate length compared to the 300 μm used here. In 2002, Tayrani [6] introduced another class E amplifier MMIC, which exhibited 13 dB gain and a peak power added efficiency of 90% at 3.25 GHz, but again required a device of 1000 μm total gate length, and a bias voltage of 12 V, which is not attractive for hand-held mobile devices. These results together with a number of HBT design performances are compared against each other in Table 2 (empty fields mean that the authors did not specify the respective parameter).

Next, the ability to directly control the output power level of the class E amplifier via its DC bias voltage was characterised (Fig. 7). Increasing the bias voltage from 0.5 to 4 V, the output power level could be varied by 14 dB. Efficiency and power added efficiency (PAE) vary over this range, e.g. PAE from about 45–100%; however, these values are still high compared to conventional linear amplifiers, e.g. class A or B, which loose efficiency following an exponential law when operated in power back-off mode [9]. Figure 7 shows that over the bias voltage range 0.5–4 V we can control the amplitude of the class E amplifier from 6.7 to 20.6 dBm without unduly changing its power added efficiency. The measurements were limited to a maximum bias voltage of 5 V owing to the maximum rating of the drain-to-source RF voltage of 7 V for the OMMIC device used.

In Fig. 7, for this operating mode of very low power levels and very high efficiencies, the resulting DC currents are becoming very small, and hence hard to measure accurately, as indicated by the increasing size of the error bars in Fig. 7, thus the indication is that efficiency is generally better that 90%.

Figure 8 shows a plot of efficiency, PAE, and gain against frequency. As can be seen, the circuit maintains an

Table 2: Comparison of recent class E amplifier designs

	QUB	Nagle	Tayrani	Grebennikov *et al.*	Koller *et al.*
Device	pHEMT	pHEMT	pHEMT	HBT	HBT
L_g	0.3 mm	12 mm	1 mm	n/a	n/a
P_{out}	21 dBm	32 dBm	23 dBm	33 dBm[1]	35 dBm[1]
Gain	27 dB	9.5 dB	15 dB	33 dB	–
η	96%	53%	–	57%	71%
PAE	94%	49%	90%	47%	63%
Frequency	870 MHz	900 MHz	3.25 GHz	1.8 GHz	900 MHz
V_{cc}	2 V	3.3 V	12 V	3.5 V	3.6 V
Year	2004	2001 [3]	2002 [6]	2003 [10]	2003 [11]

[1]Multi-stage design

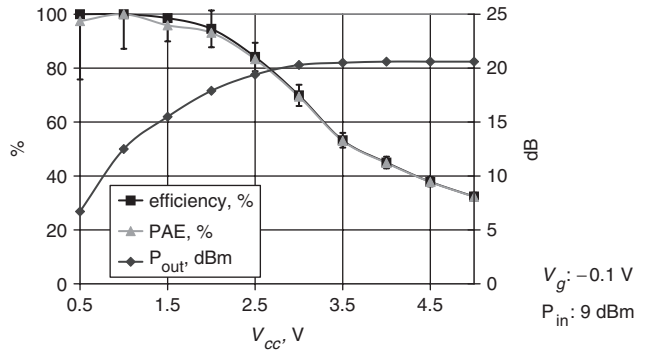

Fig. 7 *Efficiency and output power against bias voltage of class E amplifier*

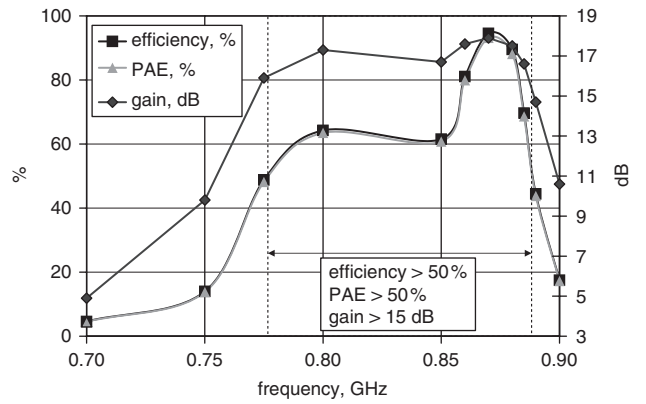

Fig. 8 *Efficiency and gain against frequency*

efficiency and power added efficiency of more than 50%, and a gain of more than 15 dB over 11.5% bandwidth.

5 Conclusions

In this work, what we believe to be the first practical demonstration of a voltage-driven class E power amplifier circuit has been given. A consequence of our work has been to show that voltage-driven class E amplifiers are best suited for small devices, hence low-power MMIC implementation for applications where high efficiency is essential. The operation of the new circuit has been explained, and the concept examined by the means of simulation, and measurement.

A prototype hybrid MIC version of the circuit was built and measured. The circuit exhibited very good performance, with 27 dB maximum gain, 21 dBm maximum output power, 96% maximum drain efficiency, and 94% maximum power added efficiency. The circuit uses a single $6 \times 50\,\mu m$ ED02AH pHEMT device, and to our knowledge these are the best results achieved to date with this size of device operated in class E mode.

6 Acknowledgments

The authors gratefully acknowledge TDK UK, TDK Ireland, and EPSRC under grant EP/C002083/1 for funding this project, Alan Black and Dr. Neil Buchanan for help with the assembly of the MIC hybrids, and Celeritek UK Ltd., – Belfast for carrying out most of the wire bonding work. The work described in this paper is the subject of British Patent Application No. 0404121.6, filed 25 February 2004.

7 References

1 Sokal, N.O., and Sokal, A.D.: 'High-efficiency tuned switching power amplifier', U.S. Patent 3,919,656, United States Patent Office, November 1975
2 Razavi, B.: 'Microelectronics, RF communications engineering and emerging technologies series' (Prentice Hall, Upper Saddle River, NJ, USA, 1998), Chap. 9, pp. 298–325
3 Nagle, P., Burton, P., Heaney, E., and McGrath, F.: 'A linear and efficient wide-bandwidth handset RF transmitter'. European Conf. on Wireless Technology, 2001, pp. 181–184
4 Cripps, S.C.: 'RF power amplifiers for wireless communications' (Artech House, Inc., Norwood, MA, USA, 1999)
5 Anholt, R.E.: 'Electrical and thermal characterization of MESFETs, HEMTs, and HBTs' (Artech House, Inc., Norwood, MA, USA, 1995)
6 Tayrani, R.: 'A broadband monolithic S-band class-E power amplifier'. IEEE Radio Frequency Integrated Circuits (RFIC) Symp. Dig., Seattle, WA, USA, June 2002, pp. 53–56
7 Raab, F.H.: 'Idealized operation of the class E tuned power amplifier', *IEEE Trans. Circuits Syst.*, 1977, **CAS-24**, (12), pp. 725–735
8 'Supplement to IEEE standard for IT, part 11' IEEE Standard 802.11b-99, 2005
9 Asbec, P.M., Larson, L.E., and Galton, I.G.: 'Synergistic design of dsp and power amplifiers for wireless communications', *IEEE Trans. Microw. Theory Tech.*, 2001, **49**, (11), pp. 2163–2169
10 Grebennikov, A., Jäger, H., and Weigel, R.: 'High-efficiency class E monolithic HBT power amplifiers for wireless applications'. 6th European Conf. on Wireless Technology, Munich, Germany, 2003, pp. 313–316
11 Koller, R., Stelzer, A., Abt, K.-H., Springer, A., and Weigel, R.: 'A class-E GSM-handset PA with increased efficiency'. 33rd European Microwave Conf., Munich, Germany, 2003, pp. 257–260